Supporting Information Appendix
For
Stability and metallization of solid oxygen under high pressure

Sabri F. Elatresh, and Stanimir A. Bonev
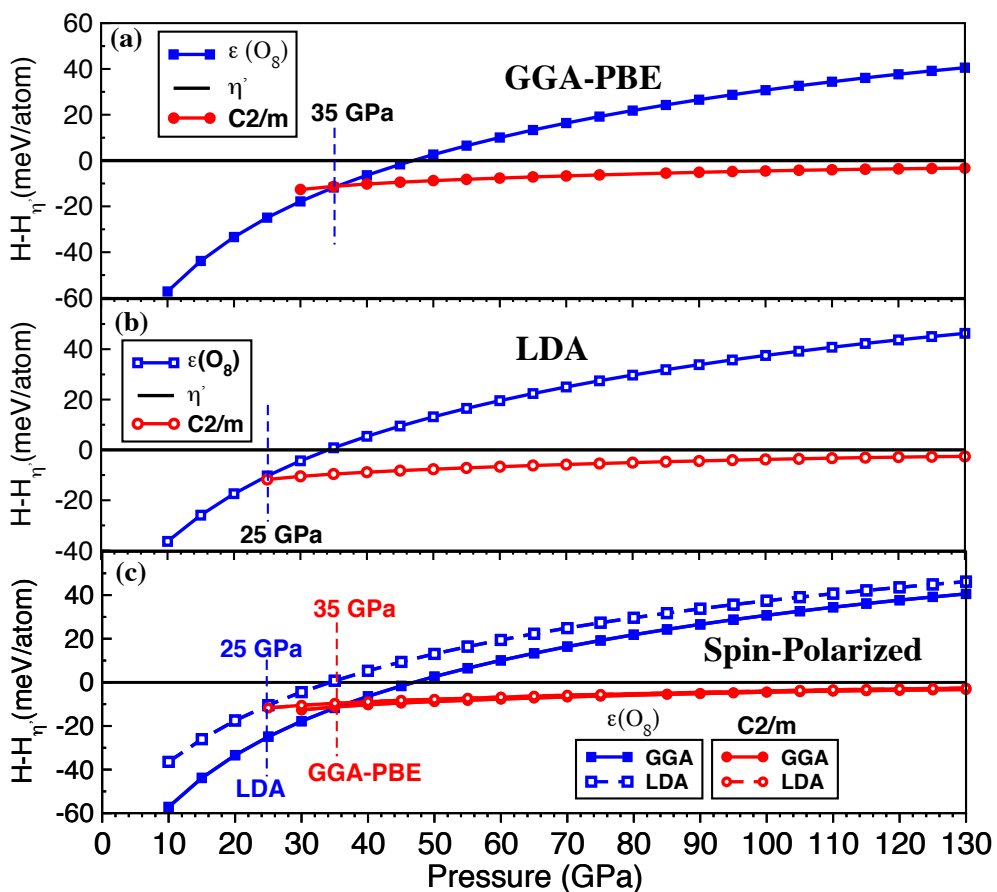
Fig. S1: (Color online) Enthalpies of the $\varepsilon(O_8)$ and $\zeta(C_2/m)$ oxygen structures relative to η' computed within the (a) GGA, (b) LDA, and (c) spin polarized LDA and GGA at 0 K. In all cases, $\zeta(C_2/m)$ is stable in the experimental stability range of $\varepsilon(O_8)$.
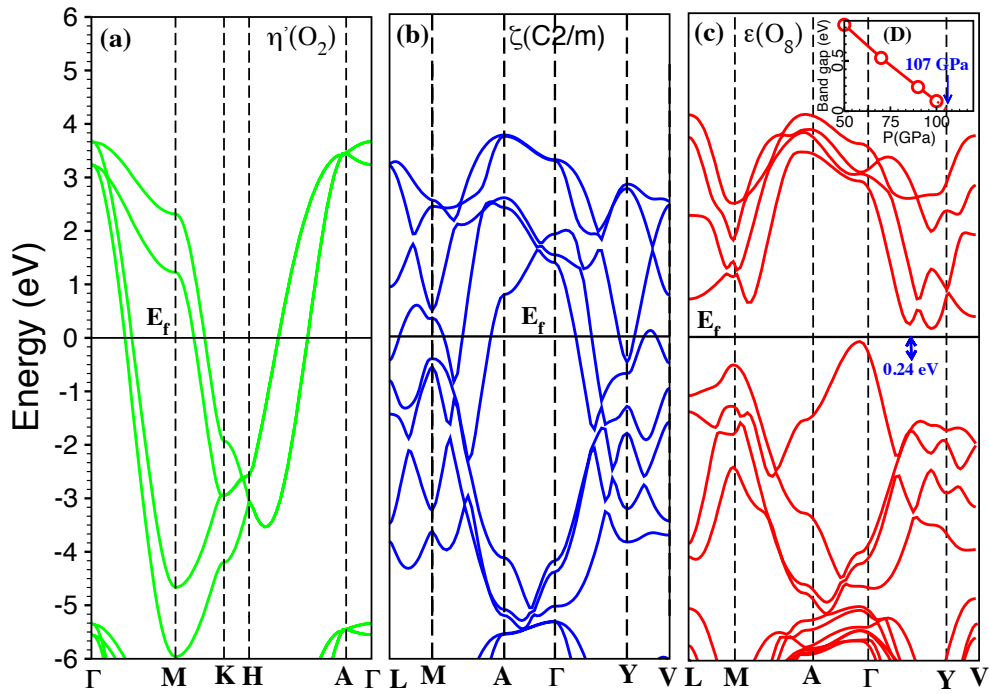
Fig. S2: Electronic band structures of solid oxygen at 90 GPa for the (a) η', (b) ζ (C_2/m), and (c) $\varepsilon(O_8)$ phases calculated within the HSE06 approximation. The inset, (D), shows the band gap of $\varepsilon(O_8)$ as a function of pressure.
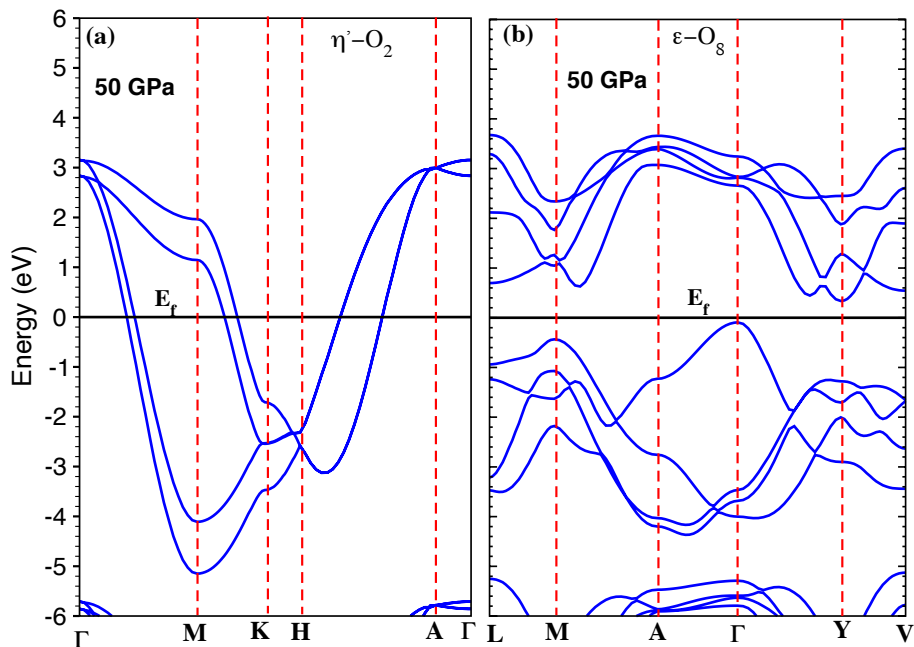
Fig. S3: Electronic band structures of solid oxygen at 50 GPa for the (a) η' and (b) $\varepsilon(O_8)$ phases calculated within the HSE06 approximation.
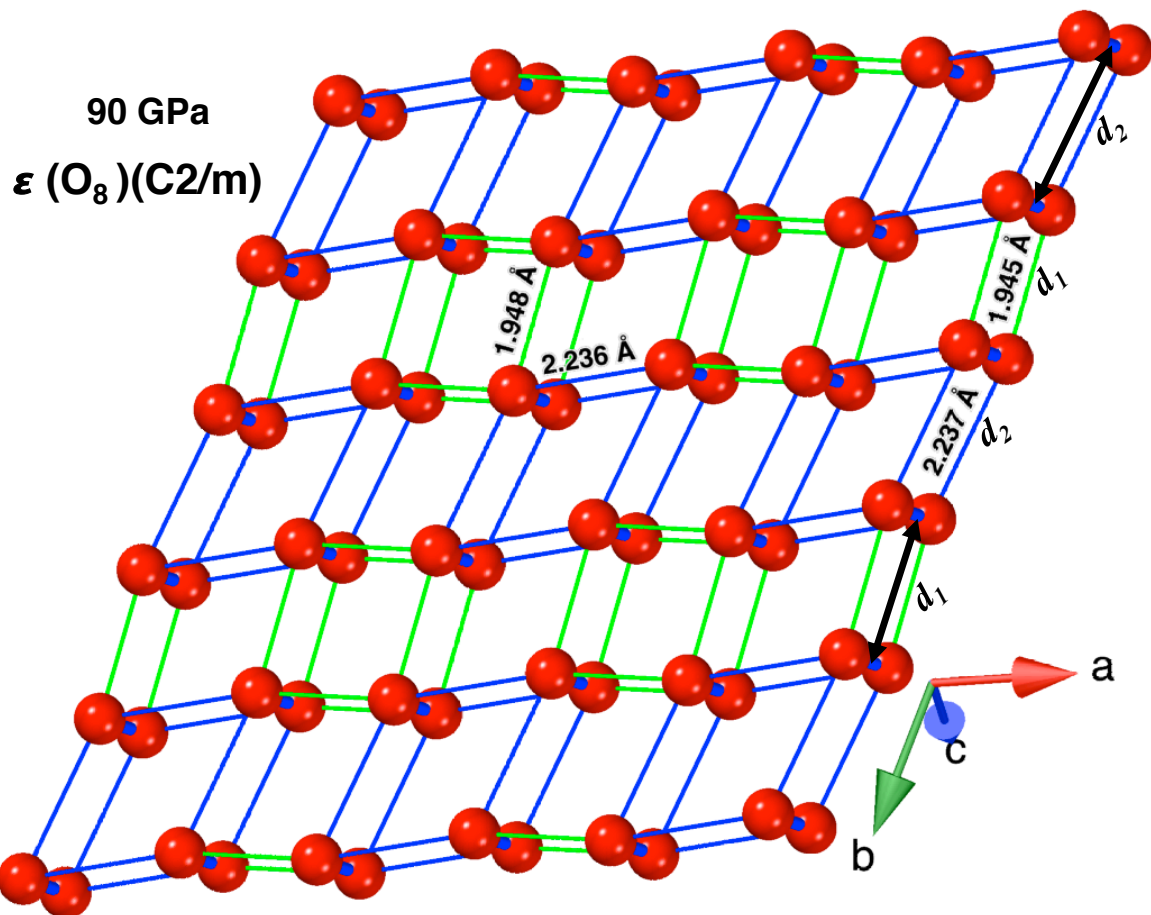
Fig. S4: (Color online) Primitive cell of the $\varepsilon(O_8)$ phase of solid oxygen at 90 GPa in the C_2/m crystal group. The intermolecular d_1 (intracell) and d_2 (intercell) distances are shown.
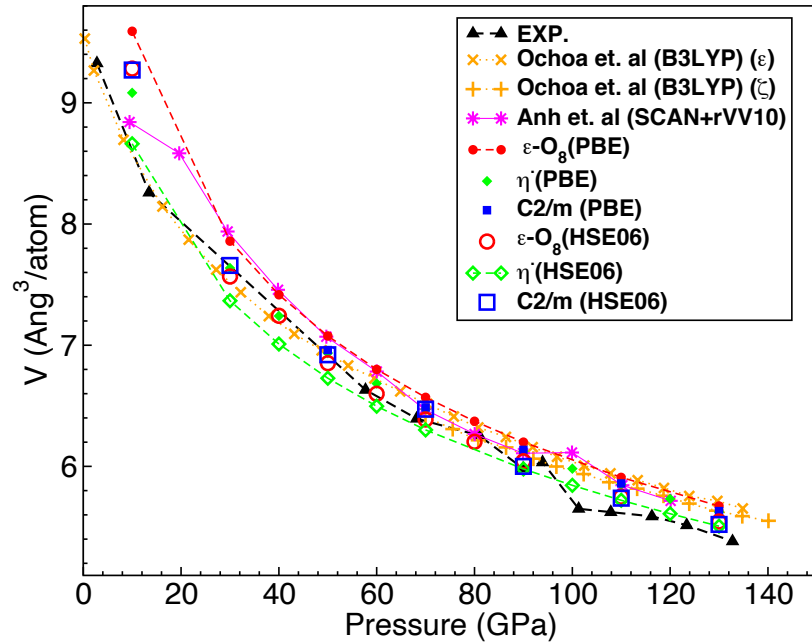
Fig. S5: (Color online) Specific volumes of the $\varepsilon(O_8)$, ζ (C_2/m), and η' phases of oxygen as a function of pressure from structural optimizations within the GGA-PBE and HSE06 approximations.
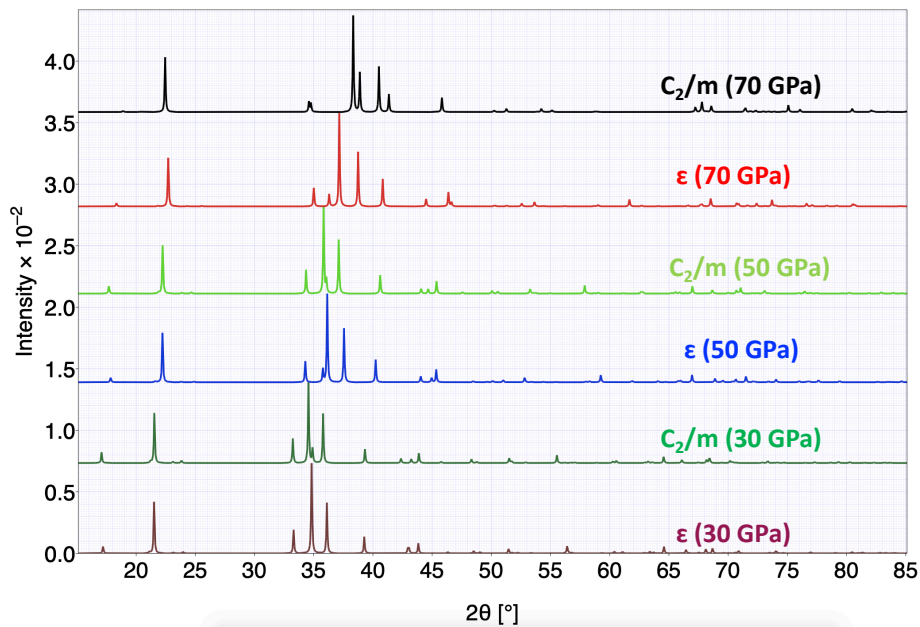
Fig. S6: Calculated X-ray diffraction spectra (for wavelength 1.213 Å) from structural optimizations (HSE06) for the $\varepsilon(O_8)$ and C_2/m oxygen structures at 30, 50 and 70 GPa.
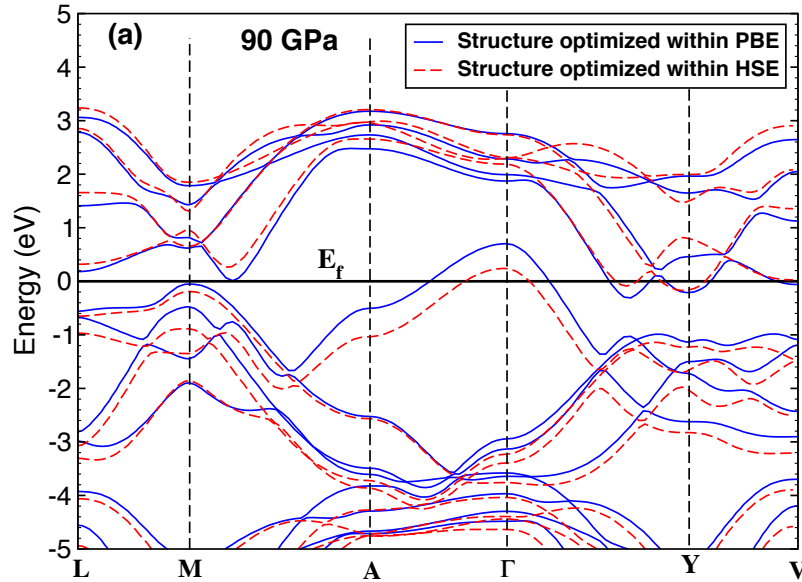
Fig. S7: Electronic band structure calculations within GGA-PBE for the $\varepsilon(O_8)$ oxygen structure optimized using GGA-PBE and HSE06. The differences originate in the resulting different O_2 bond lengths and slightly different unit cell shapes between the two exchange approximations.
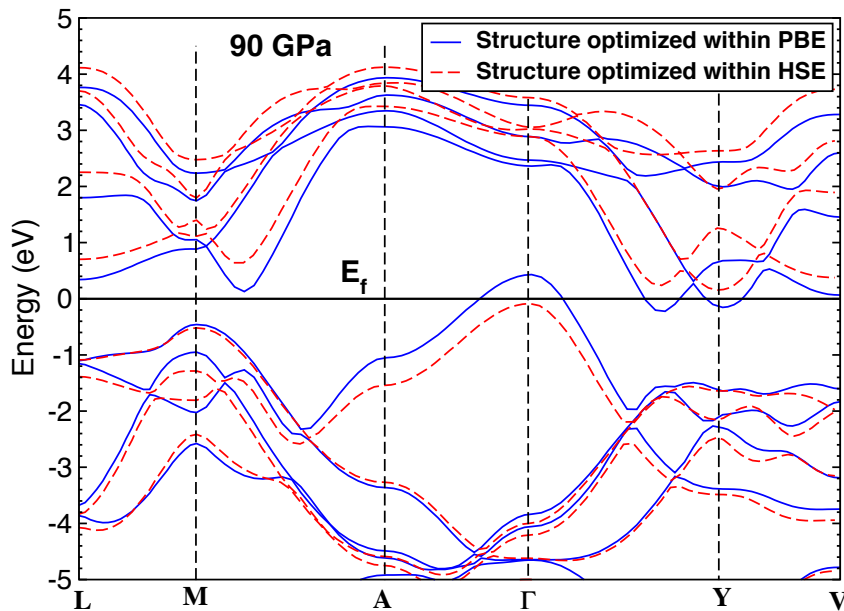
Fig. S8: Electronic band structure calculations within HSE06 for the $\varepsilon(O_8)$ oxygen structure optimized using GGA-PBE and HSE06. The differences originate in the resulting different O_2 bond lengths and slightly different unit cell shapes between the two exchange approximations.
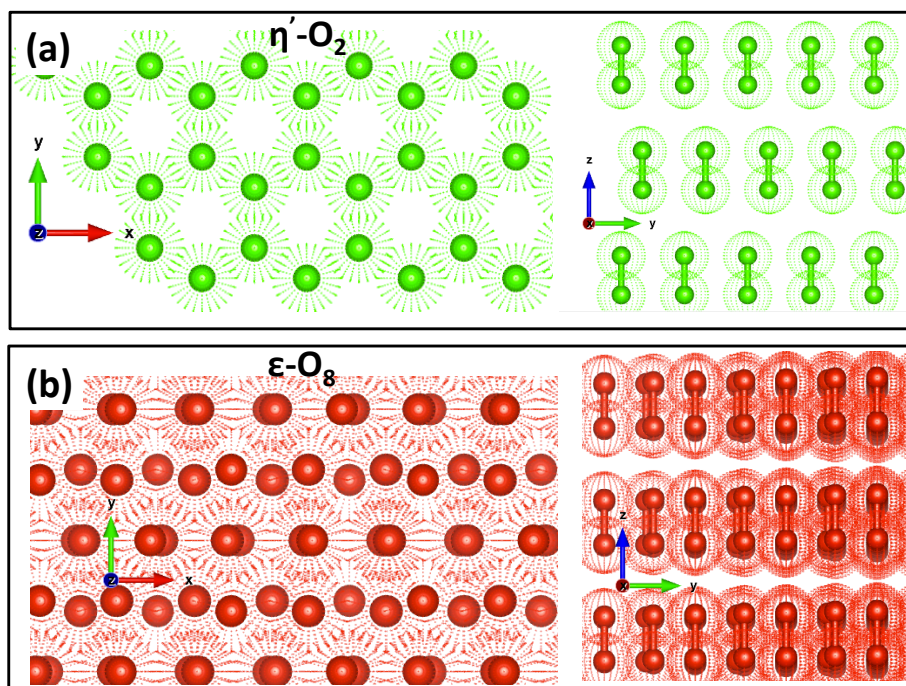
Fig. S9: Normal view along z and x axis for (a) the η′ (b) ε(O₈) phase.
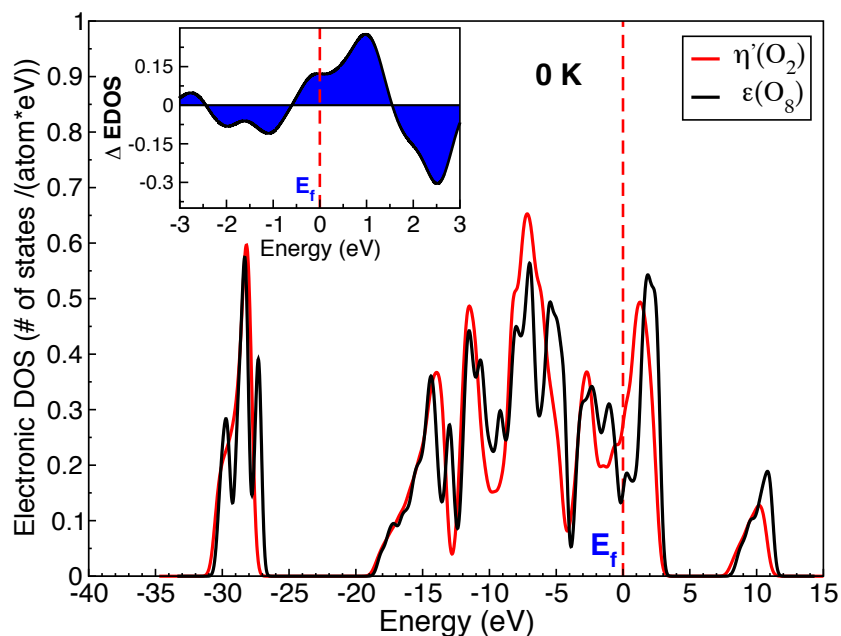
Fig. S10: Electronic density of states (EDOS) of the $\varepsilon(O_8)$ and η' oxygen structures at 0 K and ~ 50 GPa calculated within GGA-PBE. The dashed vertical lines indicate the location of the Fermi energy. The inset shows the EDOS difference (ΔEDOS = EDOS (η')-EDOS ($\varepsilon(O_8)$)).
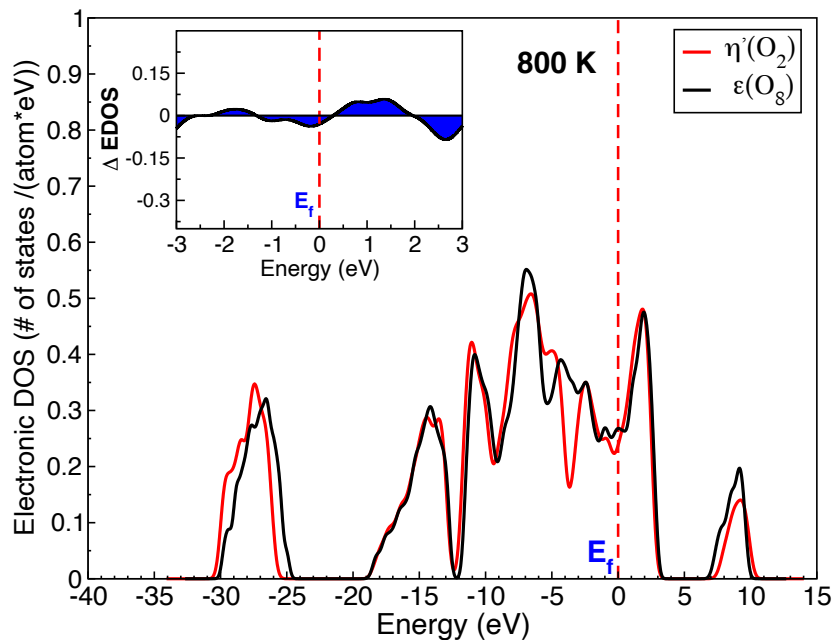
Fig. S11: Electronic density of states of the $\varepsilon(O_8)$ and η' oxygen structures at ~ 50 GPa averaged along a molecular dynamics trajectory at 800 K, calculated within GGA-PBE. The dashed vertical lines indicate location of the Fermi energy. The Inset shows the EDOS difference (ΔEDOS = EDOS (η')-EDOS ($\varepsilon(O_8)$)).